JOURNAL OF MATERIALS SCIENCE 20 (1985) 1901–1919

Review
Effect of defect structure on the electrical conduction mechanism in metallic thin films

C. R. TELLIER
Laboratoire de Chronométrie, Electronique et Piézoélectricité, Ecole Nationale Supérieure de Mécanique et des Microtechniques, La Bouloie, Route de Gray, 25030 Besançon Cédex, France

Thin metal films can be deposited in a number of different ways. As a result several types of defects or impurities are frozen in the film. In most practical cases films exhibit grain boundaries which play a decisive role in transport properties. This paper reviews the advances that have been made during the last five years in the field of theoretical description of electronic scattering at grain boundaries.

Analytical expressions for the transport parameters (such as resistivity, temperature coefficient of resistivity and thermopower) of columnar, monocrystalline and polycrystalline films are derived. Care has been taken to give linearized equations for the transport phenomena. Methods for extracting grain parameters are outlined. Special attention is focused on correlated size effects.

Imperfection or impurity effects on the film resistivity and thermopower are considered. Methods for determining the energetic parameters U and V and the component S_I of the thermopower associated with imperfections are proposed.

Special emphasis is placed on procedures for identifying imperfections by simultaneous study of the restructuration processes induced by thermal ageing and of the changes in transport parameters on ageing.

1. Introduction

Thin films are imperfect in an infinity of ways. It is usual to classify the types of imperfections by their dimensionality even if the result for electronic transport properties, i.e. a reduction of electronic conductivity, is crudely the same whatever the type of imperfection. Generally we distinguish [1]:

1. Point defects such as vacancies, interstitials or impurities.
2. Line imperfections such as dislocations.
3. Surfaces of imperfections such as grain boundaries or stacking faults.

Structural studies of metal films [2–13] have revealed that often films exhibit grained structures; both columnar-like [6–10] or fine-grained [11–13] structures have been identified. Resistivity recovery experiments [4, 7, 14–27] have been interpreted, in most cases, in terms of annihilation of point defects (vacancies or interstitials) [4, 14–19] or dislocations [14, 15, 20, 21] as well as in terms of an increase of the average grain size [8, 18, 19–24] or of mechanical reordering of the top surface of the film [4, 25–28].

Until 1968 theoretical work was devoted essentially [29–37] to the study of the geometrical limitation of the mean free path by external surfaces. In the last decade interest in electronic scattering by other imperfections has been revived,

0022–2461/85 $03.00 + .12 © *1985 Chapman and Hall Ltd.*

but among the imperfections frozen in films during the deposition process only the effect of electronic scattering at grain boundaries has been treated using simplifying assumptions [37–43].

The purpose of this paper is to present the relevant descriptions of electronic scattering at grain boundaries. In general, the paper is based on a detailed discussion of grain-boundary effects which are connected with the nature of the grains.

Most of the existing theories use a rule which states that if a single relaxation time τ_j can be defined for each type of scatterer (phonons, external surfaces or grain boundaries), the resultant relaxation time τ_f is given by:

$$\frac{1}{\tau_f} = \sum_j \frac{1}{\tau_j} = \frac{1}{\tau_0} + \frac{1}{\tau_s} + \frac{1}{\tau_g} \tag{1}$$

where 0, s and g refer respectively to phonons, external surfaces and grain boundaries.

The contribution of defects other than grain boundaries is generally analysed in terms of Matthiessen's rule [37]: the contributions to resistivity due to other imperfections (ρ_i) and to the above three types of scatterers (ρ_f) are additive and the total resistivity of the film can thus be written as

$$\rho_f^* = \rho_f + \sum_i \rho_i \tag{2}$$

It must be pointed out that in thin films the simultaneous electronic scattering at external surfaces and grain boundaries cannot be separated. In this paper the effect of external surfaces is described in the framework of Cottey's model [30]. The mean free path $\lambda_s(\theta)$ related to the external surface scattering is, for the geometry of the model (Fig. 1), given by

$$\lambda_s(\theta) = \frac{d}{\cos\theta \, \ln(1/p)} \tag{3}$$

where d is the film thickness.

The reflection coefficient p is defined as the fraction of incident carriers at any angle θ to the surface normal which are specularly scattered at the surface. In simplest theories the specularity parameter p is assumed to be independent of the angle of incidence θ. More sophisticated models [33–37] are based on the angular dependence as well as on the surface roughness dependence of the reflection coefficient. In this paper we deal with a constant parameter p.

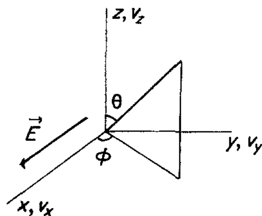

Figure 1 The geometry of the model.

2. Grain-boundary models

In the light of the results of structure analysis, films can be conveniently divided into three categories:

1. Polycrystalline films, which exhibit fine-grained structure and have an average grain diameter D_g that always remains smaller than the film thickness d.
2. Monocrystalline films, in which the average grain sizes D_{gx} and D_{gy} evaluated in the two orthogonal directions are found to be exactly equal to or greater than the film thickness.
3. Columnar films, with grains extended in the vertical direction.

A unidimensional model of grain boundaries was first proposed by Mayadas and Shatzkes [38] to describe electronic scattering at grain boundaries in monocrystalline or polycrystalline films. In this model the grains are represented by two or three arrays of planar boundaries with perfectly smooth surfaces so that only the boundaries perpendicular to the applied electric field act as operative scatterers.

However in many cases the boundary surfaces are not so perfect and the result can be achieved by a multidimensional representation of the grain boundaries [41–43]. It must be pointed out that numerical evaluation of the polycrystalline or monocrystalline film resistivity in terms of these multidimensional models has shown [37] that the Mayadas and Shatzkes model does not markedly deviate from the multidimensional models over a large range of thicknesses (discrepency less than 7%). Hence we can restrict our interest to multidimensional representations of grain boundaries.

In terms of these multidimensional models the grain-boundary scatterers in monocrystalline or columnar films are represented (Fig. 2a) by two arrays of planar boundaries with rough surfaces respectively perpendicular to the x- and y-axes (bidimensional model). In polycrystalline films three arrays oriented perpendicular to the x-, y-

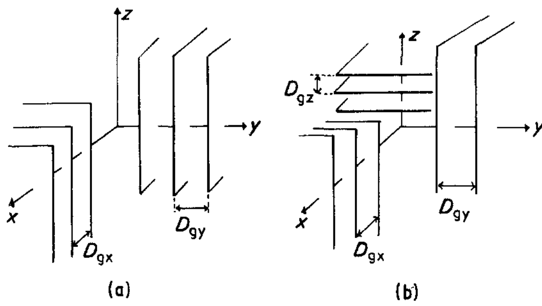

Figure 2 The grain-boundary models: (a) representation of columnar or monocrystalline films; (b) representation of polycrystalline films.

and z-axes respectively (Fig. 2b) are assumed to cause the resistivity increase. Whatever the multidimensional representation of the grain boundaries, the mathematical treatment is based on common physical arguments. It consists of assuming that the statistical scattering properties of the grain boundaries can be described by two physical parameters: the average grain size D_g and the transmission coefficient t through grain boundaries. The tranmission coefficient t is defined as the fraction of electrons transmitted through the potentials that represent the grain boundaries with conservation of the electron wave vector **K**. The remainder are diffusely scattered and no longer contribute to the current [41–43].

The probability that an electron travels a distance L before suffering a collision at a grain boundary is given by

$$\mathscr{P}_i = t^{N_i} \quad i = x,y,z \tag{4}$$

where N_i is the number of successive transmissions through the boundaries oriented perpendicular to the i-direction.

If N_i is large, i.e. if the transmission coefficient t is not far from unity, the probability $\mathscr{P}_i$ can be rewritten in terms of an exponential function of the mean free path λ_i related to the grain-boundary scattering process:

$$\mathscr{P}_i = \exp(-L/\lambda_i) \tag{5}$$

From the geometry of the models and since from a statistical point of view we are concerned with grains having an average grain size D_{gi}, the number of planar boundaries N_i can be expressed as

$$N_i = \frac{L}{D_{gi}} \chi_i \tag{6}$$

where the geometrical parameter χ_i depends on the orientation of the grain boundary array:

$$\chi_x = |\sin\theta|\,|\cos\phi| \tag{7}$$

$$\chi_y = |\sin\theta|\,|\sin\phi| \tag{8}$$

$$\chi_z = |\cos\theta| \tag{9}$$

Thus for the multidimensional models the total probability is readily expressed in terms of the two following alternative relations:

$$\mathscr{P} = t^{\Sigma_i N_i} = \exp\left(-L\sum_i \frac{1}{\lambda_i}\right) \tag{10}$$

where the sums are concerned with the x- and y-directions in the case of monocrystalline or columnar films and with the three directions (x,y,z) in the case of polycrystalline films.

If the scatterers act independently of each other it is possible to define a single relaxation time or mean free path for each type of scatterer, so that the mean free path λ_f describing the combined effects of background, grain-boundary and external surface scattering may be written as

$$\frac{1}{\lambda_f} = \frac{1}{\lambda_0} + \frac{1}{\lambda_s} + \sum_i \frac{1}{\lambda_i} \tag{11}$$

Note here that strictly speaking λ_0 is related to electron–phonon scattering. However, thin films are imperfect in different ways and it is often convenient to choose a mean free path λ_0 which refers to background scattering processes and thus concerns the scattering mechanisms occurring in the volume other than the grain-boundary scattering.

Introducing Equation 3 into Equation 11 the total mean free path λ_{fp} for polycrystalline films with cubic-like structure is given by:

$$\lambda_{fp}^{-1} = \lambda_0^{-1}\{1 + C^2\nu^{-1} + |\cos\theta|\,[(1-C)\nu^{-1} + \mu^{-1}]\} \tag{12}$$

defining for convenience the grain parameter ν and the surface parameter μ respectively as

$$\nu = D_g\left[\lambda_0 \ln\left(\frac{1}{t}\right)\right]^{-1} \tag{13}$$

$$\mu = d\left[\lambda_0 \ln\left(\frac{1}{p}\right)\right]^{-1} \tag{14}$$

This simple result has been obtained with the use of the approximate relation

$$|\cos\Psi| + |\sin\Psi| \approx 4/\pi = C \tag{15}$$

Assuming that in monocrystalline and columnar films the grain boundaries consist of two arrays with the same average spacing D_g, the total mean free path, λ_{fm} or λ_{fc}, for such thin films is readily found to be expressed by the same formula:

$$\lambda_{fm}^{-1}, \lambda_{fc}^{-1}, = \lambda_0^{-1} [1 + C^2 v^{-1} + |\cos\theta| (\mu^{-1} - Cv^{-1})] \quad (16)$$

Taking into account that several experimental works [37, 44–50] have been interpreted by assuming that in monocrystalline films the average grain size is exactly equal to the film thickness, it must be pointed out that in the following section we have chosen to treat the monocrystalline film in the special case where $D_g \approx d$.

3. Grain-boundary effects on transport properties

The transport properties of a thin film are obviously sensitive to grain-boundary scattering. In this section we look at the changes in transport parameters caused by both external surface and grain-boundary scattering. The mathematical treatment is carried our under the assumption that the free-electron model is applicable. Thus the electron energy ϵ is given by

$$\epsilon = \tfrac{1}{2} mv^2 \quad (17)$$

where m is the isotropic electron mass.

The general expressions for the current density J_x and heat flux Q_x in a thin metal film subjected to an electric field E_x and a temperature gradient $\partial T/\partial x$ in the x-direction are [1]:

$$J_x = -2e\left(\frac{m}{h}\right)^3 \int f_1 v_x \, d^3 v \quad (18)$$

and

$$Q_x = 2\left(\frac{m}{h}\right)^3 \int f_1 (\epsilon - \epsilon_F) v_x \, d^3 v \quad (19)$$

respectively, where e is the absolute electron charge, v_x is the x-component of electron velocity v, ϵ_F is the Fermi energy, h is Planck's constant and f_1 represents the deviation from the equilibrium distribution function f_0.

We determine the function f_1 by solving the Boltzmann transport eqution with the approximation that all collision processes can be described in terms of the unique relaxation time $\tau_{fj} = \lambda_{fj} v^{-1}$:

$$f_1 = \frac{e}{m} \tau_{fj} \frac{\partial f_0}{\partial v_x} \left[E'_x + \frac{1}{e}\left(\frac{\epsilon - \epsilon_F}{T}\right) \frac{\partial T}{\partial x}\right] \qquad j = \mathrm{c, m, p} \quad (20)$$

E'_x is the effective electric field [1] given by

$$E'_x = E_x + \frac{1}{e} \frac{\partial \epsilon_F}{\partial x} \quad (21)$$

Introducing Equation 20 into Equations 18 and 19 and using polar coordinates (v, θ, ϕ), it is then easily shown that J_x and Q_x can be expressed in terms of coefficients K_n:

$$J_x = e^2 K_0 E'_x + \frac{e}{T} K_1 \frac{\partial T}{\partial x} \quad (22)$$

and

$$Q_x = -eK_1 E'_x + \frac{K_2}{T} \frac{\partial T}{\partial x} \quad (23)$$

with

$$K_n = -\frac{4\pi m}{h^3} \int_0^\infty \epsilon (\epsilon - \epsilon_F)^n \frac{\partial f_0}{\partial \epsilon} \, d\epsilon \int_0^\pi \lambda_{fj}(\theta, \epsilon) \times \sin^3\theta \, d\theta \, |_{\epsilon = \epsilon_F} \qquad n = 0, 1, 2 \quad (24)$$

If we consider the macroscopic Equations 22 and 23, then we readily have for the transport parameters, i.e. the electrical conductivity σ_f, the absolute thermopower S_f and the thermal conductivity κ_f, the expressions

$$\sigma_f = e^2 K_0 \quad (25)$$

$$S_f = -\frac{1}{eT} \frac{K_1}{K_0} \quad (26)$$

and

$$\kappa_f = \frac{1}{T}\left(K_2 - \frac{K_1^2}{K_0}\right) \quad (27)$$

If we write the energy dependence of the background relaxation time in the form [51]

$$\tau_0 = \tau_b \epsilon^q \quad (28)$$

where τ_b is a constant and q a number, the integral K_n can be easily evaluated by means of the formula [1]

$$-\int_0^\infty G(\epsilon) \frac{\partial f_0}{\partial \epsilon} \, d\epsilon = G(\epsilon_F) + \frac{(\pi k_B T)^2}{6} G''(\epsilon_F) + \ldots \quad (29)$$

which is obtained by expanding the function $G(\epsilon)$ in a Taylor series about $\epsilon = \epsilon_F$ and k_B is Boltzmann's constant.

Retaining the first term only in the expression for K_0 the film conductivity takes the general form [42, 43]

$$\frac{\sigma_{fj}}{\sigma_0} = \frac{3}{2} \frac{1}{b_j} [a_j - \tfrac{1}{2} + (1 - a_j^2) \ln(1 + a_j^{-1})] = \frac{3}{2} \frac{1}{b_j} f(a_j) \qquad j = \mathrm{c, m, p} \quad (30)$$

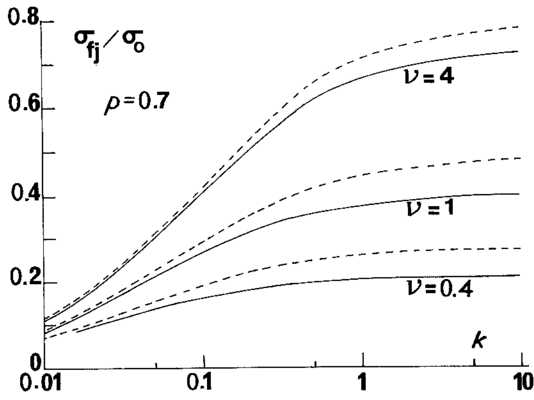

Figure 3 The reduced conductivity σ_{fj}/σ_0 plotted against the reduced thickness k for polycrystalline (full curves) and columnar (broken curves) films and for different values of the grain parameter ν.

where σ_0 is the background conductivity. As above the subscripts c, m and p refer respectively to columnar, monocrystalline and polycrystalline films.

The effect of grain structure is seen through the a_j and b_j coefficients. Effectively this analysis leads to

$$a_{\mathrm{c,m}} = (1 + C^2 v^{-1}) b^{-1}_{\mathrm{c,m}} \tag{31}$$

with

$$b_{\mathrm{c,m}} = \mu^{-1} - C v^{-1} \tag{32}$$

for columnar or monocrystalline films and to

$$a_{\mathrm{p}} = (1 + C^2 v^{-1}) b_{\mathrm{p}}^{-1} \tag{33}$$

with

$$b_{\mathrm{p}} = \mu^{-1} + (1 - C) v^{-1} \tag{34}$$

for polycrystalline films.

Equation 30 can be evaluated numerically with the aid of a pocket calculator. Comparison of the reduced conductivity ratio σ_{fj}/σ_0 for polycrystalline or columnar films (Fig. 3) and monocrystalline films with $D_g \approx d$ (Fig. 4) reveals several interesting features.

1. Columnar and polycrystalline film behaviours present a formal similarity: the conductivity markedly depends on the grain parameter ν and approaches a limiting conductivity σ_{gj} in the limit of large reduced thickness $k = d/\lambda_0$ (i.e. for $\mu \to \infty$). Care must be taken if the grain-boundary conductivities σ_{gm} and σ_{gc} reduce to an identical formula

$$\frac{\sigma_{gj}}{\sigma_0} = \frac{3}{2} \frac{1}{b_{j\infty}} f(a_{j\infty}) \qquad j = \mathrm{c, p} \tag{35}$$

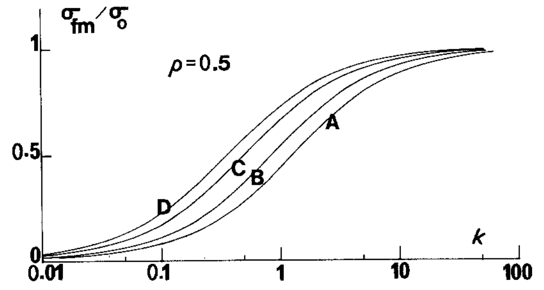

Figure 4 Plot of σ_{fm}/σ_0 against k for monocrystalline films. Curves A, B, C and D are theoretical curves for the respective t values of 0.4, 0.6, 0.8 and 0.9, and for $p =$ 0.5.

the limiting values of the parameters a_j and b_j for columnar films

$$a_{\mathrm{c}\infty} = -(\nu + C^2) C^{-1} \tag{36}$$

$$b_{\mathrm{c}\infty} = -C\nu^{-1} \tag{37}$$

differ from those for polycrystalline films

$$a_{\mathrm{p}\infty} = (1 + C^2 \nu^{-1}) b^{-1}_{\mathrm{p}\infty} \tag{38}$$

$$b_{\mathrm{p}\infty} = (1 - C)\nu^{-1} \tag{39}$$

From a crude point of view the grain-boundary scatterers limit the apparent mean free path to about the grain size.

2. Since for monocrystalline films $d \approx D_g$ or $D_g > d$, it is easy to see that when the thickness becomes infinite the film conductivity σ_{fm} reduces to the background conductivity.

3. If the grain boundaries cease to act as efficient scatterers (i.e. when the grain size tends to infinity and/or the transmission coefficient to unity), the multidimensional film conductivities coincide with the Cottey conductivity [30] as expected for films in which grain-boundary scattering no longer contributes to the current.

Returning now to Equation 24 and considering the case of an energy-dependent background relaxation time (Equation 28), it clearly appears that for $n = 1$ and 2 the integral remains elementary. This gives

$$K_1 = \frac{3}{2} \frac{\sigma_0}{e^2} \frac{(\pi k_B T)^2}{3\epsilon_F} \left(\left(q + \frac{1}{2}\right) \frac{g(a_j)}{b_j^2} + \frac{f(a_j)}{b_j} \right)$$
$$j = \mathrm{c, m, p} \tag{40}$$

with

$$g(a_j) = a_j^{-1} - 2 + 2a_j \ln(1 + a_j^{-1})$$
$$j = \mathrm{c, m, p} \tag{41}$$

and

$$K_2 = \frac{(\pi k_B T)^2}{3} K_0 \qquad \text{for } \pi k_B T \epsilon_F^{-1} \ll 1 \tag{42}$$

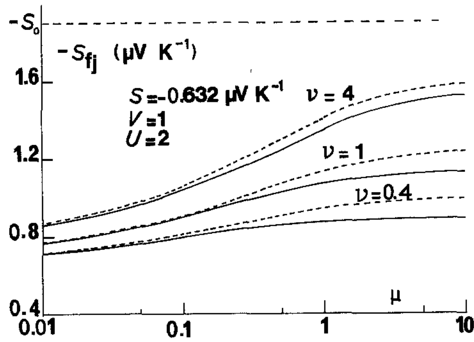

Figure 5 Thermopower of columnar (broken curves) and polycrystalline (full curves) films as a function of the surface parameter μ.

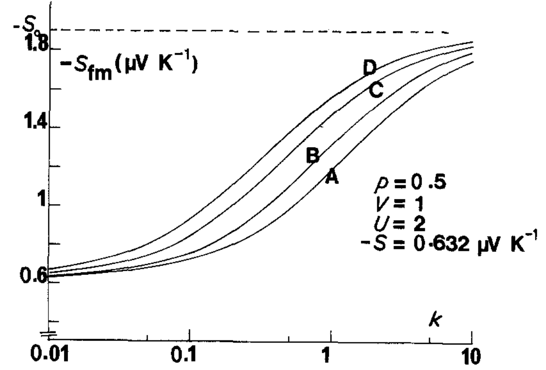

Figure 6 Monocrystalline film thermopower S_{fm} against the reduced thickness k. Curves A, B, C and D are theoretical curves for the respective t values of 0.4, 0.6, 0.8 and 0.9, and for $p = 0.5$.

Returning to the formal expressions for the conductivity σ_{fj}, thermopower S_{fj} and thermal conductivity κ_{fj}, substitution of Equations 30, 40 and 42 into the respective Equations 26 and 27 gives

$$S_{fj} = -\frac{(\pi k_B)^2 T}{3e\epsilon_F}\left(1 + (q + \tfrac{1}{2})\frac{1}{b_j}\frac{g(a_j)}{f(a_j)}\right)$$

$$j = \mathrm{c, m, p} \qquad (43)$$

and

$$\kappa_{fj} = \frac{(\pi k_B)^2 T}{3}\left(\frac{3}{2}\frac{\sigma_0 f(a_j)}{e^2 b_j}\right) \qquad \text{for } \pi k_B T \epsilon_F^{-1} \ll 1 \qquad (44)$$

revealing that for $\pi k_B T \epsilon_F^{-1} \ll 1$ and at ambient temperature the grain-boundary effects on thermal conductivity are identical to effects on electrical conductivity [52]. Thus in this section we limit our attention to electrical conductivity and thermopower.

The thermoelectric power of columnar and polycrystalline films is shown in Fig. 5 as a function of μ. Fig. 5 reveals at once that we have here the situation described for film conductivity: the same conclusions can be brought in the limit of very large μ or ν parameters. In studying the effect of grain-boundary scattering on monocrystalline film thermopower (Fig. 6) we also inevitably see a close analogy between electrical conductivity and thermopower behaviours.

At this point it may be remarked that, of course, the true Fermi surfaces are surely non-spherical and the proportionality between the square of the electron velocity, v^2, and the area, $\mathscr{A}$, of constant-energy surfaces is then inaccurate. Moreover some authors [1, 51] have suggested that thermopower depends sensitively on the details of the Fermi surface. For these reasons it is usual [1, 37, 51] to evaluate the thermopower by introducing the parameter

$$V = \left(\frac{\partial \ln \mathscr{A}}{\partial \ln \epsilon}\right)_{\epsilon = \epsilon_F} \qquad (45)$$

which must changed markedly with distortions in the Fermi surface and the parameter

$$U = \left(\frac{\partial \ln \lambda_0}{\partial \ln \epsilon}\right)_{\epsilon = \epsilon_F} \qquad (46)$$

which depends on the energy dependence of the relaxation time.

Note that if the free-electron model holds, the terms V and U are readily identified with respectively 1 and $q + \frac{1}{2}$.

It must be kept in mind that provided $\epsilon_F \gg k_B T$ we may use the relation

$$S_f = S\left(\frac{\partial \ln \sigma_f(\epsilon)}{\ln \epsilon}\right)_{\epsilon = \epsilon_F} \qquad (47)$$

which is still valid for a distorted Fermi surface. Here for convenience we define

$$S = -\frac{(\pi k_B)^2 T}{3e\epsilon_F} \qquad (48)$$

In terms of $\mathscr{A}$ and λ_0 we can write the film conductivity as

$$\sigma_{fj} = \sigma_0 F_j(\lambda_0) \sim \mathscr{A}\lambda_0 F_j(\lambda_0) \qquad (49)$$

with $F_j(\lambda_0) = b_j^{-1} f(a_j)$. Hence the film thermopower now reads

$$S_{fj} = S\left[V + U\left(1 + \frac{\partial \ln F_j(\lambda_0)}{\partial \ln \lambda_0}\right)\right]_{\epsilon = \epsilon_F} \qquad (50)$$

making use of Equation 47. Note that the evaluation of the thermopower with this alternative leads to an equation of universal applicability. $(\partial \ln F_j/\partial \ln \lambda_0)_{\epsilon=\epsilon_F}$ is now the basic function to be calculated. This receives attention in a later section.

4. Correlated grain-boundary effects

It may be of interest (see Sections 5 and 6) to compare grain-boundary effects on resistivity, its temperature coefficient (TCR) and other transport coefficients such as thermopower since one expects that imperfections do not affect the various transport parameters in the same manner [1, 14].

Data on film TCR are in most cases [14, 46, 49, 53–58] interpreted in terms of size effects by considering the following usual assumptions [37, 59, 60].

1. The rigid band model of metals is valid.
2. The number of conduction electrons per unit volume is temperature independent in the experimental range.
3. The thermal expansion of the grain and the film thickness are negligible with respect to that of the mean free path.

If we retain these assumptions and further neglect the thermal expansion mismatch between the film and its substrate, logarithmic differentiation of the general Equation 49 leads to

$$\frac{\beta_{fj}}{\beta_0} = 1 + \frac{\partial \ln F_j(\lambda_0)}{\partial \ln \lambda_0} \qquad j = c, m, p \qquad (51)$$

since from assumptions 1 and 2 we have for the bulk TCR

$$\beta_0 = -\frac{d \ln \lambda_0}{dT} = -\frac{d \ln \sigma_0}{dT} \qquad (52)$$

and since the film TCR is defined by

$$\beta_{fj} = -\frac{d \ln \sigma_{fj}}{dT} \qquad (53)$$

Returning to Equation 30 and noting that the parameters ν and μ are inversely proportional to λ_0 we obtain after some calculation:

$$\frac{\beta_{fj}}{\beta_0} = \frac{1}{b_j}\frac{g(a_j)}{f(a_j)} \qquad j = c, m, p \qquad (54)$$

Hence at once we identify $\partial \ln F_j(\lambda_0)/\partial \ln \lambda_0$ with $b_j^{-1}\, g(a_j)/f(a_j) - 1$.

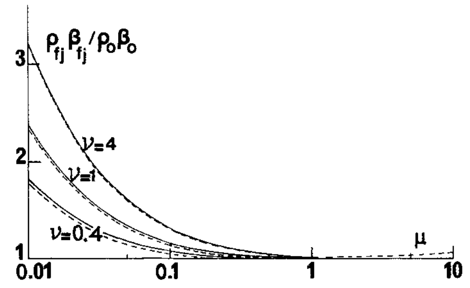

Figure 7 The reduced product, resistivity × TCR, i.e. $\rho_{fj}\beta_{fj}/\rho_0\beta_0$, of columnar (broken curves) and polycrystalline (full curves) films as a function of μ.

Evaluation of the product, resistivity × TCR, shows (Fig. 7) that for columnar or polycrystalline films the relation

$$\beta_{fj}\rho_{fj} \approx \beta_{gj}\rho_{gj} \approx \beta_0\rho_0 \qquad j = c, p \qquad (55)$$

is satisfied at large reduced thickness, $k = d/\lambda_0$, range (i.e. $k > 0.1$). This can be interpreted by the fact that grain-boundary effects do not vary with temperature.

Moreover the size effects are less accentuated in monocrystalline films (Fig. 8) since the relation [60]

$$\beta_{fm}\rho_{fm} \approx \beta_{fm}\rho_0 \qquad (56)$$

is valid until k reaches values greater than 0.01. Hence from Equations 55 and 56 similar size effects on resistivity ratio, ρ_{fj}/ρ_∞, and TCR ratio, β_∞/β_{fj}, are predicted.

We now proceed with thermopower. Comparing Equations 50 and 51 gives [60, 61]

$$S_{fj} = S\left(V + U\frac{\beta_{fj}}{\beta_0}\right) \qquad j = c, m, p \quad (57)$$

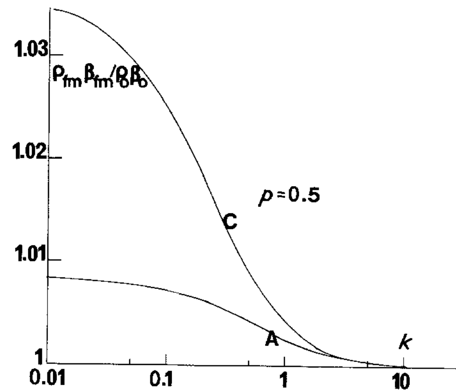

Figure 8 Variations in the reduced product $\rho_{fm}\beta_{fm}/\rho_0\beta_0$ with the reduced thickness k. Curves A and C are theoretical curves for the respective t values of 0.4 and 0.8, and for $p = 0.5$.

showing that, as suggested by Thompson [62], for external surface effects, the size effects on thermopower, due here to both grain boundaries and surfaces, are intimately connected with size effects on TCR. Note also that as the Relation 56 is valid for monocrystalline films in the very large thickness range, the size effects on monocrystalline thermopower must be correlated with size effects on electrical conductivity as predicted by the equation [63]

$$S_{\mathrm{fm}} = S\left(V + U\frac{\sigma_{\mathrm{fm}}}{\sigma_0}\right) \tag{58}$$

where the conductivity ratio replaces the TCR ratio in Equation 57.

Moreover the multidimensional grain-boundary models can be used [64, 65] to calculate the transport properties of grained films subjected to an electric field (E_x, E_y, 0) in the plane of the film and a transverse magnetic field (0, 0, H), contrary to the Mayadas and Shatzkes model for which the problem of calculating the conductivity is only tractable when a one-dimensional array of grain boundaries distributed perpendicular to the electric field is considered.

The result can be achieved [64, 65] by expressing the Boltzmann equation under the combined action of the applied electric and magnetic fields within the framework of previous analysis [66, 67] and then by expressing the deviation f_1 in terms of two functions which do not explicitly depend on the components v_x and v_y of the electron velocity. This analysis leads after tedious calculations to complicated analytical expressions. Fortunately a correlation exists between the size effects on the Hall coefficient $R_{\mathrm{Hf}j}$ and the product, resistivity × TCR, i.e. $\rho_{\mathrm{f}j}\beta_{\mathrm{f}j}$ [37],

$$R_{\mathrm{Hf}j}/R_{\mathrm{H0}} \approx \rho_{\mathrm{f}j}\beta_{\mathrm{f}j}/\rho_0\beta_0 \qquad j = \mathrm{c, m, p} \tag{59}$$

where R_{H0} is the Hall coefficient of the bulk material.

Equation 59 is accurate to describe the Hall effect in polycrystalline or columnar films of any thickness since only slight deviations from this relation are obtained for high values of the magnetic field (i.e. $H = 1$ T). Moreover for monocrystalline films the Hall coefficient is not appreciably affected by grain-boundary effects: when the transmission coefficient t reaches values larger than 0.4 the size effect on R_{Hfm} vanishes whatever the strength of the magnetic field. Since the Hall effect in monocrystalline films can be described from the Relationship 59 this result agrees with the theoretical predictions related to the product, resistivity × TCR.

At this point it must be remarked [1] that, like thermopower, the Hall coefficient is a sensitive function of the Fermi surface and can be strongly modified [14, 68] in the presence of defects. Hence Formula 59 is of greatest importance in the practical study of grain-boundary effects when systematic study of the electrical resistivity, its TCR and Hall effect are undertaken simultaneously.

5. Experimental determination of transport parameters

On one hand, it appears from Sections 3 and 4 that the resistivity and TCR of grained films depend mainly on three essential parameters, namely D_{g}, p and t, which are known to change with deposition conditions and annealing [3, 8, 12, 16, 18–28, 69–72]. On the other hand, the parameters U and V describing respectively the energy dependence of the mean free path and Fermi surface area are affected by large concentrations of imperfections; distortion of the Fermi surface [15, 57, 68, 72, 73] as well as modification of the energy dependence of the relaxation time [15, 57, 68, 72] in the presence of imperfections have been examined. Hence it is essential to determine these important parameters from experimental data for the understanding of effects of grain boundaries or imperfections. In particular it seems that graphical determinations of these parameters are convenient ways of studying structural effects. Hence in this section we deal with some graphical methods of analysis, some of them requiring the establishment of linearized expressions for the transport parameters $\sigma_{\mathrm{f}j}$ and $\beta_{\mathrm{f}j}$.

The difficulty then is to find a linearization where the variables μ and ν can be separated in order to fit experimental data on the resistivity or its TCR with a formula with the variables (D_{g}, t) and p as adjustable parameters. Unfortunately such accurate linearization can be derived only for columnar or polycrystalline films.

Returning to Equation 30 it is easy to prove that in the limiting case $a_j \gg 1$ the film conductivity and resitivity take the two alternative forms:

$$\sigma_{\mathrm{f}j}/\sigma_0 \approx (a_j b_j)^{-1}\left(1 - \tfrac{3}{8}a_j\right) \tag{60a}$$

$$j = \mathrm{c, m, p}$$

$$\rho_{\mathrm{f}j}/\rho_0 \approx a_j b_j \left(1 + \tfrac{3}{8} a_j\right) \qquad (60\mathrm{b})$$

whose ν and μ ranges of applicability can differ.

Using approximate Relation 60a for $|b_{\mathrm{p}}^{-1}| \ll 1$ and $|a_{\mathrm{p}}| \gg 1$ the polycrystalline film conductivity reduces to

$$\frac{\sigma_{\mathrm{fp}}}{\sigma_0} \approx \left(1 + \frac{C^2}{\nu}\right)^{-1} \left[1 - \tfrac{3}{8}\left(\frac{1}{\mu} + \frac{1-C}{\nu}\right)\left(1 + \frac{C^2}{\nu}\right)\right]^{-1} \qquad (61)$$

This readily shows that for an infinitely thick polycrystalline film we have

$$\frac{\sigma_{\mathrm{gp}}}{\sigma_0} = \left(1 - \tfrac{3}{8}\,\frac{1-C}{\nu(1 + C^2\nu^{-1})}\right)\left(1 + \frac{C^2}{\nu}\right)^{-1} \qquad (62)$$

Combining Equations 61 and 62 gives the resitivity ratio in the limiting form [74]

$$\frac{\rho_{\mathrm{fp}}}{\rho_{\mathrm{gp}}} \approx 1 + \frac{3}{8\mu}\left[1 + \frac{C^2}{\nu} - \tfrac{3}{8}\left(\frac{1-C}{\nu}\right)\right]^{-1} \qquad (63)$$

Equation 63 suggests clearly that the polycrystalline film resistivity can be described by a linear asymptotic expression in the form

$$\rho_{\mathrm{fp}}/\rho_{\mathrm{gp}} = 1 + k^{-1}\ln(1/p)\, M_{\mathrm{p}}(\nu) \qquad (64)$$

Adjusting the function $M_{\mathrm{p}}(\nu)$ to make the range of applicability of Equation 64 larger ($\mu > 0.1$ with $0.1 \leqslant \nu \leqslant 4$) leads to a relation [37]

$$M_{\mathrm{p}}(\nu) = (4.7\nu^{-1} + 3)^{-1} \qquad (65\mathrm{a})$$

which is not really very different from the relation

$$M_{\mathrm{p}}(\nu) = \left\{\tfrac{3}{8}\left[1 + \frac{1}{\nu}\left(C^2 - \frac{3(1-C)}{8}\right)\right]\right\}^{-1} \qquad (65\mathrm{b})$$

derived directly from the Approximation 63.

The TCR ratio $\beta_{\mathrm{gp}}/\beta_{\mathrm{fp}}$ can be obtained by a similar treatment. However returning to Equation 55 the result is immediate:

$$\beta_{\mathrm{gp}}/\beta_{\mathrm{fp}} = 1 + k^{-1}\ln(1/p)\, M_{\mathrm{p}}(\nu) \qquad (66)$$

Since for monocrystalline films we always have $D_{\mathrm{g}} > d$, we can at once write the asymptotic Equation 60b as:

$$\frac{\rho_{\mathrm{fm}}}{\rho_0} = 1 + \frac{3}{8\mu} + \frac{C}{\nu}\left(C - \tfrac{3}{8}\right) \qquad (67\mathrm{a})$$

which indicates that for $d \approx D_{\mathrm{g}}$ the monocrystalline film resistivity can be represented by the linear relation [60]

$$\rho_{\mathrm{fm}}/\rho_0 \approx 1 + k^{-1}\,[C_2\ln(1/p) + C_1\ln(1/t)]$$
$$= 1 + k^{-1}M_{\mathrm{m}}(p, t) \qquad (67\mathrm{b})$$

In order to extend the range of applicability ($k > 0.01$) of this approximate relation and to obtain a smaller deviation between the exact and approximate values of the resistivity ratio, the constants C_2 and C_1 are taken as

$$C_2 = 0.36 \qquad C_1 = 1.144 \qquad (68)$$

in relatively close agreement with the constants obtained from Equation (63).

With the aid of the Relation 52 the linear expression:

$$\beta_0/\beta_{\mathrm{fm}} = 1 + k^{-1}\, M_{\mathrm{m}}(t, p) \qquad (69)$$

follows directly for the TCR ratio.

The analysis is rather fastidious for columnar films where $D_{\mathrm{g}} < d$. However a convenient procedure commences with Equation 67a which is valid for monocrystalline films and gives results in suprisingly good agreement with theoretical predictions. Noting that the resistivity of an infinitely thick colunnar films can be written as

$$\rho_{\mathrm{gc}}/\rho_0 \approx 1 + (C - \tfrac{3}{8})\,\nu > 1 \qquad (70)$$

and then combining Equations 67a and 70 yields

$$\rho_{\mathrm{fc}}/\rho_{\mathrm{gc}} = 1 + k^{-1}\ln(1/p)\, M_{\mathrm{c}}(\nu) \qquad (71)$$

with

$$M_{\mathrm{c}}(\nu) = \left\{\tfrac{8}{3}\left[1 + \frac{C}{\nu}\left(C - \tfrac{3}{8}\right)\right]\right\}^{-1} \qquad (72)$$

One finds an evidently identical asymptotic expression for the columnar TCR ratio $\beta_{\mathrm{gc}}/\beta_{\mathrm{fc}}$ whose range of applicability extends to $\mu > 0.1$ for $0.1 \leqslant \nu \leqslant 4$.

Before we deal with thermopower we pause here to examine the possibilities of graphical determination of the parameters ν and p. Equations 64 and 66 and 71 predict that a plot of $k\rho_{\mathrm{f}j}$ ($j = \mathrm{c, p}$) or $k/\beta_{\mathrm{f}j}$ against k should yield a straight line with slope $\rho_{\mathrm{g}j}$ or $1/\beta_{\mathrm{g}j}$ and ordinate intercept $\rho_{\mathrm{g}j}M_j(\nu)\ln(1/p)$ or $M_j(\nu)\ln(1/p)/\beta_{\mathrm{g}j}$. Since the parameter ν can be evaluated from the slope by means of Equation 35 it is then easy to deduce separately the value of the specularity parameter p from the intercept provided that structural study has revealed the exact structure (cubic-like or columnar-shaped) of grains.

From Equation 67b it appears that such a useful treatment cannot be undertaken for monocrystalline films. Interpretation of exper-

imental data in the form $\rho_{fm}k$ against k allows only the evaluation of the function $M_m(t, p)$ and it is very difficult to make an accurate choice between the possible set of (t, p) values. However provided that some additional structural studies were made one can obtain some interesting information on the changes in the p and t coefficients under various annealing and deposition conditions.

Since in this section we collect the results related to graphical determination of structure-dependent parameters we are inevitably concerned with the U and V parameters. It is often appropriate to define the difference in thermopower as

$$\Delta S_{gj} = S_{fj} - S_{gj} \qquad (73)$$

Turning to Equation 57, taking into account that the thermopower of an infinitely thick film can be written as

$$S_{gj} = S\left(V + U\frac{\beta_{gj}}{\beta_0}\right) \qquad (74)$$

and combining Equations 57 and 74 gives the general relation [61]

$$\Delta S_{gj} = SU\left(\frac{\beta_{gj}}{\beta_{gj}} - 1\right)\frac{\beta_{gj}}{\beta_0} \qquad (75)$$

Note that Equation 75 applies also for monocrystalline film, it is sufficient to identify β_{gj} with β_0 (i.e. index $g \approx 0$). Consequently a plot of ΔS_{gj} against β_{fj}/β_{gj} should yield a straight line with an abscissa intercept of unity and an ordinate intercept of $-SU(\beta_{gj}/\beta_0)$. Since β_{gj} (or β_0 for monocrystalline films) can be easily evaluated from data reporting the thickness dependence of TCR of grained films of well defined structure, the value of U can be graphically determined.

It may be also useful to consider the TCR ratio β_{fj}/β_{gj} dependence of the thermopower ratio S_{fj}/S_{gj} by means of the formula

$$\frac{S_{fj}}{S_{gj}} = \frac{SV}{S_{gj}} + \left(\frac{SU}{S_{gj}}\frac{\beta_{gj}}{\beta_0}\right)\frac{\beta_{fj}}{\beta_{gj}} \qquad (76)$$

where for monocrystalline films S_{gm} and β_{gm} must be respectively taken as S_0 and β_0. It must be pointed out that S_g, β_g (or S_0, β_0 for moncrystalline films), U and V may be regarded as "intrinsic" parameters if the structure of grained films does not vary with thickness. Hence a plot of S_{fj}/S_{gj} against β_{fj}/β_{gj} should yield a straight line with an ordinate intercept SV/S_{gj} and a slope of (SU/S_{gj}) (β_{gj}/β_0) which must pass through the point $(S_{fj}/S_{gj} = 1,\ \beta_{fj}/\beta_{gj} = 1)$. It thus appears that analysis of thermopower data in the form S_{fj}/S_{gj} against β_{fj}/β_{gj} allows the graphical determination of both U and V.

Note also that the monocrystalline film thermopower must satisfy Equation 58; thus if TCR data are not available for monocrystalline films it is possible in the light of Equation 58 to interpret the thermopower data in terms of conductivity data. The analysis and methods of graphical determination of energy-dependent parameters U and V are quite similar to above procedures. We must only replace in Equation 75 and 76 the TCR ratio and to take care that for monocrystalline films we have to identify σ_{gj} with σ_0. Since the experimental measure of β_{fm} can be subjected to quite significant errors due to the slight values of β_f[32, 37] and in some cases to the mismatch in thermal expansion coefficients of the film and its substrate [37, 75–77], this alternative procedure surely leads to a more accurate determination of the parameters U and V [78].

Since the theoretical grain and thickness dependence of the TCR ratios can be approximated by linear relations an alternative method for evaluating U and V is to use the asymptotic expressions

$$S_{fj} = S\left[V + U\frac{\beta_{gj}}{\beta_0}\left(1 + \frac{\ln p^{-1}}{k}M_j(\nu)\right)^{-1}\right]$$

$$j = \mathrm{c, p} \qquad (77)$$

or

$$S_{fm} = S\{V + U[1 + k^{-1}M_m(t, p)]^{-1}\} \qquad (78)$$

for thermopower.

Equation 77 presents no difficulty: since the factor $M_j(\nu)\ln(1/p)$ takes very small values, Equation 77 can be rewritten as

$$S_{fj} = S\left[V + U\frac{\beta_{gj}}{\beta_0}\left(1 - \frac{\ln p^{-1}}{k}M_j(\nu)\right)\right]$$

$$j = \mathrm{c, p} \qquad (79)$$

But care must be taken in the case of monocrystalline films since Equations 67b and 68 indicate that the constant $M_m(t, p)$ can exhibit values higher than 1.5 as observed in recent experiments [50, 79, 80]. Hence we are restricted to the two following limiting cases [81]:

1. When $M_m(t, p)/k \ll 1$, i.e. when grain-boundary scattering does not markedly contribute

to the resistivity, expansion of Equation 78 gives to lowest order

$$S_{\mathrm{fm}} \approx S_0 - SUM_{\mathrm{m}}(t,p)k^{-1} \qquad M_{\mathrm{m}}k^{-1} \ll 1 \qquad (80)$$

Equation 80 predicts that a plot of $S_{\mathrm{fm}}k$ against k should yield a straight line with slope S_0 and ordinate intercept $-SUM_{\mathrm{m}}(t,p)$.

2. When $M_{\mathrm{m}}(t, p)/k \gg 1$, i.e. when grain boundaries act as efficient scatterers, the consistent linear relation is

$$S_{\mathrm{fm}} \approx SV + SUk/M_{\mathrm{m}}(t,p) \qquad k/M_{\mathrm{m}}(t,p) \ll 1 \qquad (81)$$

which shows that valuable information on the U and V parameters can be obtained by plotting thermopower data in the form S_{fm} against k.

The choice of the accurate plot is conveniently determined by simultaneous resistivity measurements.

6. Role of imperfections and effect of annealing

Before we deal with impurities or imperfections other than grain boundaries it may be of interest to return to theoretical approximate expressions of grained film resistivity. From Equations 67a and b it appears at once that the thin monocrystalline film resistivity obeys Matthiessen's rule:

$$\rho_{\mathrm{fm}} \approx \rho_0 + \rho^*_{\mathrm{gm}} + \rho_{\mathrm{s}} \qquad (82)$$

where ρ^*_{gm} and ρ_{s} are respectively the resistivities due to grain boundary and external surface scattering.

Rerranging the asymptotic Equations 63 and 71 one now shows that the polycrystalline or columnar film resistivity can be described by an additive resistivities rule

$$\rho_{\mathrm{f}j} \approx \rho_{\mathrm{g}j} + \rho_{\mathrm{s}} \qquad j = \mathrm{c, p} \qquad (83)$$

where the phonon contribution ρ_0 is included in the infinitely thick film resistivity $\rho_{\mathrm{g}j}$, which if the grain boundaries do not act as very efficient scatterers can be rewritten in the form

$$\rho_{\mathrm{g}j} = \rho_0 + \rho^*_{\mathrm{g}j} \qquad j = \mathrm{c, p} \qquad (84)$$

satisfying Matthiessen's rule.

Further considering the additional contribution ρ_{I} of other imperfections to the total film resistivity, $\rho^*_{\mathrm{f}j}$, it follows that

$$\rho^*_{\mathrm{fm}} \approx \rho_0 + \rho^*_{\mathrm{gm}} + \rho_{\mathrm{s}} + \rho_{\mathrm{I}} = \sum_i \rho_i \qquad (85)$$

and

$$\rho^*_{\mathrm{f}j} \approx \rho_{\mathrm{g}j} + \rho_{\mathrm{s}} + \rho_{\mathrm{I}} = \sum_i \rho_i \qquad j = \mathrm{c, p} \qquad (86)$$

The total film thermopower defined by the relation

$$S^* = -S\left(\frac{\mathrm{d}\ln\rho^*}{\mathrm{d}\ln\epsilon}\right)_{\epsilon=\epsilon_{\mathrm{F}}}$$

can now be given by the Nordheim–Gorter rule [51]

$$S^*_{\mathrm{f}j} = \rho^{*-1}_{\mathrm{f}j}\sum_i \rho_i S_i \qquad (87)$$

where we have made use of the relation

$$S_i = -S\left(\frac{\partial\ln\rho_i}{\partial\ln\epsilon}\right)_{\epsilon=\epsilon_{\mathrm{F}}} \qquad (88)$$

for the thermopower due to the ith scattering process. Accordingly we write

$$S^*_{\mathrm{fm}} = \rho^{*-1}_{\mathrm{fm}}(\rho_0 S_0 + \rho_{\mathrm{s}}S_{\mathrm{s}} + \rho^*_{\mathrm{gm}}S^*_{\mathrm{gm}} + \rho_{\mathrm{I}}S_{\mathrm{I}}) \qquad (89)$$

and

$$S^*_{\mathrm{f}j} = \rho^{*-1}_{\mathrm{f}j}(\rho_{\mathrm{s}}S_{\mathrm{s}} + \rho_{\mathrm{g}j} + \rho_{\mathrm{I}}S_{\mathrm{I}}) \qquad j = \mathrm{c, p} \qquad (90)$$

We limit here our attention to the difference $\Delta S^*_{\mathrm{g}j}$ between the film and the "perfect" bulk material (i.e. the "perfect" infinintely thick film). Applying the Nordheim–Gorter rule and rearranging Equations 85 and 89 gives four alternative expressions for the monocrystalline difference $\Delta S^*_{0\mathrm{m}}$

$$\Delta S^*_{0\mathrm{m}} = -S_0 + \rho^{*-1}_{\mathrm{fm}}(\rho_0 S_0 + \rho_{\mathrm{s}}S_{\mathrm{s}} + \rho^*_{\mathrm{gm}}S^*_{\mathrm{gm}} + \rho_{\mathrm{I}}S_{\mathrm{I}}) \qquad (91\mathrm{a})$$

$$\Delta S^*_{0\mathrm{m}} = (S_{\mathrm{I}} - S_0) + \rho^{*-1}_{\mathrm{fm}}[\rho_0(S_0 - S_{\mathrm{I}}) + \rho_{\mathrm{s}}(S_{\mathrm{s}} - S_{\mathrm{I}}) + \rho^*_{\mathrm{gm}}(S^*_{\mathrm{gm}} - S_{\mathrm{I}})] \qquad (91\mathrm{b})$$

$$\Delta S^*_{0\mathrm{m}} = (S_{\mathrm{s}} - S_0) + \rho^{*-1}_{\mathrm{fm}}[\rho_0(S_0 - S_{\mathrm{s}}) + \rho^*_{\mathrm{gm}}(S^*_{\mathrm{gm}} - S_{\mathrm{s}}) + \rho_{\mathrm{I}}(S_{\mathrm{I}} - S_{\mathrm{s}})] \qquad (91\mathrm{c})$$

$$\Delta S^*_{0\mathrm{m}} = (S^*_{\mathrm{gm}} - S_0) + \rho^{*-1}_{\mathrm{fm}}[\rho_0(S_0 - S^*_{\mathrm{gm}}) + \rho_{\mathrm{s}}(S_{\mathrm{s}} - S^*_{\mathrm{gm}}) + \rho_{\mathrm{I}}(S_{\mathrm{I}} - S^*_{\mathrm{gm}})] \qquad (91\mathrm{d})$$

and only three alternative expressions for the columnar and polycrystalline difference $\Delta S^*_{\mathrm{g}j}$ since Equation 86 involves only three resistivity terms

$$\Delta S^*_{\mathrm{g}j} = -S_{\mathrm{g}j} + \rho^{*-1}_{\mathrm{f}j}(\rho_{\mathrm{g}j}S_{\mathrm{g}j} + \rho_{\mathrm{s}}S_{\mathrm{s}} + \rho_{\mathrm{I}}S_{\mathrm{I}}) \qquad j = \mathrm{c, p} \qquad (92\mathrm{a})$$

$$\Delta S^*_{gj} = (S_s - S_{gj}) + \rho^{*-1}_{fj} [\rho_{gj}(S_{gj} - S_s) + \rho_I(S_I - S_s)] \quad (92b)$$

$$\Delta S^*_{gj} = (S_I - S_{gj}) + \rho^{*-1}_{fj} [\rho_{gj}(S_{gj} - S_I) + \rho_s(S_s - S_I)] \quad (92c)$$

The film resistivity ρ^*_{fj} is know to change with annealing. Hence in terms of Equations 91 and 92 a plot, for a given film subjected to successive annealings, of ΔS^*_{0m} or ΔS^*_{gj} against $1/\rho^*_{fj}$ should yield a straight line, as suggested by several authors [58, 82–85]. However examination of Equations 91 and 92 shows than an adequate choice for the true expressions of the slope and ordinate intercept is not clear. This will be discussed later.

Some authors [72, 73, 83, 86] have advanced arguments to suggest that the U and V parameters can vary on annealing. It must be pointed out that this interpretation has been proposed by using Equation 47 [72] or an equation derived within the framework of the Fuchs–Sondheimer model, i.e. an equation obtained by considering only the external surfaces effect [86]. From Equations 91 and 92 it thus appears that the parameters U or/and V evaluated by these authors must include terms which can be modified on annealing. It is certainly the case for the resistivities ρ_s, ρ_g and ρ_I even if the thermoelectric powers S_s, S_g and S_I can be regarded as "intrinsic" thermopowers which remain unchanged on annealing. It might be of interest to determine if the energy-dependent parameters U and V, related to the contribution S_0 in metal films, differ from those related to the thermopower of bulk pure metal, and thus to verify if the Fermi surface in metal films is distorted with regard to the Fermi surface in bulk metal.

Let us, for example, consider the case of monocrystalline films containing imperfections and exhibiting average grain sizes ($d \approx D_g$) which remain unchanged or increase very slightly following anneal, as sometimes observed in experimental work [4, 87]. In spite of this assumption the analysis must be subdivided into two limiting cases depending on the $M_m(t, p)/k$ values.

From Equations 82 and 87 it appears that the total monocrystalline thermopower may be written as

$$S^*_{fm}\rho^*_{fm} = \rho_I S_I + \rho_{fm} S_{fm} \quad (93)$$

where ρ_{fm} and S_{fm} are just the transport parameters derived in Section 5 (Equations 67, 78 and 80). Hence under the assumption of very small $M_m(t, p)/k$ the expression for S^*_{fm} becomes, after simple but rather tedious mathematical manipulations,

$$S^*_{fm} \approx S_{\infty m} + \frac{M_m(t,p)}{k} \frac{\rho_0}{\rho_0 + \rho_I}(SV - S_{\infty m}) \quad (94)$$

where $S_{\infty m}$ is

$$S_{\infty m} = (\rho_I S_I + \rho_0 S_0)(\rho_0 + \rho_I)^{-1} \quad (95)$$

and is readily identified with the thermopower of an infinitely thick film having the same microstructure as that of the thin film. Note that such a physical intepretation of Equation 95 supposes implicitly that the concentration of imperfections does not vary with thickness. Since S_∞ is connected with ρ_I care must be taken that changes in S_∞ can be induced by annealing. We see from Equation 94 that by knowing $(\rho_I + \rho_0)$ from resistivity data we can determine V by plotting S^*_{fm} data in the form $S^*_{fm}k$ against k, provided we are concerned with thickness-independent concentration of imperfections.

In the limit of large $M_m(t, p)k^{-1}$, combining Equations 67b, 79 and 93 gives

$$S^*_{fm} = SV + \frac{k}{M_m(t,p)}\left(\frac{\rho_I}{\rho_0}(S_I - SV) + SU\right) \quad (96)$$

Inspection of Equation 96 reveals that a plot of S^*_{fm} against k allows us to calculate V separately from the ordinate intercept provided that ρ_I is thickness-independent.

Since for columnar or polycrystalline films the function $\ln(1/p)M_j(\nu)k^{-1}$ also takes small values, a close analogy exists between the asymptotic Equation 94 and the following asymptotic equation

$$S^*_{fj} = S_{\infty j} + \frac{\rho_{gj}}{\rho_I + \rho_{gj}} \frac{\ln(1/p)M_j(\nu)}{k}(SV - S_{\infty j})$$

$$j = c, p \quad (97)$$

derived for films whose infinitely thick film resistivity, $\rho_{gj} + \rho_I$, differs from $\rho_0 + \rho_I$. Here the thermopower of an infinitely thick film is expressed as

$$S_{\infty j} = (S_I\rho_I + S_{gj}\rho_{gj})(\rho_I + \rho_{gj})^{-1} \qquad j = c, p \quad (98)$$

Equations 97 suggests a method to determine V

provided that the following requirements are fulfilled:

1. The contribution ρ_I can be neglected for thoroughly annealed films.

2. The changes in ρ_{gj} on annealing can be essentially attributed to increase of the grain size and the grain growth is estimated from structural studies

In these conditions we expect to determine V, for structurally well defined films, at different stages of annealing since at each stage $\rho_I + \rho_{gj}$ and $S_{\infty j}$ can be estimated from the slope of respective linear plots of $k\rho^*_{fj}$ and kS^*_{fj} against k.

It is necessary to pause here and to remark that Equations 91 and 92 are essentially concerned with a given film whose resistivity decreases on ageing. However some difficulties arise since on the one hand interpretation of data generally requires the validity of the assumption that there are no variations in S_I, S_s and S_g during annealing and on the other hand, as noted above, true quantitative results on S_I, S_s or S_g are difficult to obtain since it is physically doubtful to assume that annealing induces no changes in ρ_s or/and ρ_g. Equations 94, 96 and 97 are concerned with a set of films of various thicknesses and should provide valuable information on the energy parameter V especially when severe conditions of deposition ensure a concentration of imperfections which does not vary with thickness. Unfortunately any of the existing methods requires the use of physical assumptions which may differ from one method to another and this is not very favourable for a precise evaluation of the physical parameters V, U and S_I. We can make some progress, however, by undertaking simultaneous measurements of all the transport properties and then interpreting the data on the basis of all previous equations.

Annealing of the films results in the removal of frozen-in defects [4, 7, 14, 27]; valuable information on the restructuration mechanisms can be obtained [18, 20, 21, 23–25] if several successive annealings are performed at various temperatures. Kinetic study of the resistivity recovery during successive isothermal annealings allows us to determine the activation energy for the recovery process [18, 20, 21, 23, 25]. Moreover experiments [21, 23] have given evidence of successive recovery stages with different activation energies. By comparing the experimental values for activation energies with other values, from the literature related to the bulk specimen, the different recovery stages can generally be attributed to defined restructuration processes [21, 23]. Moreover if the calculated activation energy varies markedly with film thickness then the observed behaviour may be understood by assuming that the concentration of imperfections depends on film thickness. Structure determination during or after thermal treatment is of great interest especially when the resistivity recovery is caused by an increase of the grain size or a decrease of the surface roughness. Moreover these structural studies allow us to treat the resistivity as if related to a well defined grain model. It thus appears that some preliminary but useful information for the characterization of imperfections can be obtained from an annealing study.

An estimate of the magnitude of the contribution of imperfections to transport properties can be made by undertaking simultaneous measurements of the resisitvity, its TCR and the Hall coefficient. Only slight size effects on the Hall coefficient together with correlated size effects on Hall coefficient and the product, resistivity × TCR, characterize unambiguously metal films in which only grain-boundary and surface scattering significantly modify the bulk transport properties. Effectively if the contribution ρ_I to the resistivity is temperature-independent, a law identical to Equation 59 can hold in agreement with some experimental data [14]. Departure from the law (Equation 59) can be attributed to a very large and completely randomized concentration of impurities or other imperfections.

Study of ageing effects on thermopower at different stages can provide quantitative determination of S_I [84–86]. However, as discussed previously, it is a difficult task to evaluate this parameter precisely. Consider for example a monocrystalline film where a structural examination and an annealing study have given evidence that the grain boundaries and external surfaces are not markedly modified by the successive annealings and that only one type of imperfection contributes to the resistivity ρ_I which changes on annealing. If further a plot of ΔS^*_{0m} against $1/\rho^*_{fm}$ yields a straight line with a single slope and no intersecting straight lines as sometimes observed [84, 85], Equation 91b is then the suitable equation to use to determine the intrinsic S_I. It is now well established that Equations 91 and 92 require a lot of somewhat questionable assumptions

and allow a true quantitative evaluation of $S_{\rm I}$ in limited experimental work.

However if the conductivity $\sigma^*_{\rm fm}/\sigma_0$ or $\sigma^*_{\rm f\mathit{j}}/\sigma_{\rm g\mathit{j}}$ ratio dependence of the difference $\Delta S^*_{\rm 0m}$ or $\Delta S^*_{\rm g\mathit{j}}$ in thermopowers does not correspond to a linear law in the relatively large thickness range, it may be advanced without ambiguity that the observed behaviour is due to a thickness-dependent contribution of imperfections. It is effectively well established [37] that the contributions $\rho_{\rm s}$ and $\rho^*_{\rm gm}$ to the total resistivity $\rho^*_{\rm f\mathit{j}}$ (j = c, p) and $\rho^*_{\rm fm}$ become negligible in the limit of large thicknesses. Then for monocrystalline films any of Equations 91 reduces to

$$\Delta S^*_{\rm 0m}|_{d,\,D_{\rm g}\to\infty} \approx (S_{\rm I}-S_0)(1-\sigma^*_{\rm fm}/\sigma_0) \qquad (99)$$

and for columnar and polycrystalline films, any of Equations 92 to

$$\Delta S^*_{\rm g\mathit{j}}|_{d\to\infty} \approx (S_{\rm I}-S_{\rm g\mathit{j}})(1-\sigma^*_{\rm f\mathit{j}}/\sigma_{\rm g\mathit{j}}) \qquad (100)$$

Equation 99 and 100 indicate that:

1. In the presence of a large concentration of imperfections (i.e. for $\sigma^*_{\rm fm}/\sigma_0$ or $\sigma^*_{\rm f\mathit{j}}/\sigma_{\rm g\mathit{j}} \ll 1$), ΔS^* becomes zero only if respectively $S_{\rm I} \approx S_0$ or $S_{\rm I} \approx S_{\rm g\mathit{j}}$.
2. In the general case where the imperfection concentration is thickness-dependent the plot of ΔS^* against $\sigma^*_{\rm fm}/\sigma_0$ or $\sigma^*_{\rm f\mathit{j}}/\sigma_0$ exhibits marked departure from a straight line.

Simultaneously interpreting thermopower data in terms of size effects can provide additional information on the nature of imperfections by means of evaluation of the parameters U and V and then $S_{\rm I}$. As discussed earlier, the values of V calculated for different isothermal annealings can be considered true quantitative results only if (returning for example to the case of monocrystalline films) the films exhibit perfect monocrystalline structure after subsequent annealing and a thickness-independent concentration of imperfections during annealing. If moreover annealing results in no growth of grains ($d \approx D_{\rm g}$) and no significant difference between the observed value of V and the bulk value, it is possible to evaluate the imperfection thermopower $S_{\rm I}$ for different annealing stages and for a given set of films. Further the fact that $S_{\rm I}$ varies on annealing can be attributed to the removal of different imperfections in the successive annealing stages, in particular if this behaviour is confirmed by the experimental determination of different activation energies for the various recovery stages.

If the grain size increases on annealing, Equations 94 and 96 must be modified (i.e. $k^{-1}C_2$ must be replaced by $\lambda_0 C_2/D_{\rm g}$) to separate the grain-boundary and external surface contributions. Interpretation of data then becomes rather complex since annealing can result in both growth of grains and correlated decrease of $\rho^*_{\rm gm}$. Hence, as for columnar and polycrystalline films, careful investigation of the grain structure during annealing becomes necessary to undertake a correct estimate of the parameters $S_{\rm I}$, V and U.

These few examples clearly indicate that identification of imperfections in thin films remains a difficult task. However a qualitative estimate can be made provided that simultaneous studies of size effects in various transport parameters are undertaken for as-deposited films and for films annealed at different temperatures. The more numerous the experimental data, the more accurate become the qualitative and sometimes quantitative identification of imperfections.

7. Experimental results

There are many results on thin-film resistivity or/and its TCR which may be understood in terms of multidimensional grain-boundary models [37]. In this section only some of the earlier published results on transport properties of thin films are discussed.

Early results on the resistivity of aluminium films [55] were found to be in agreement with a grain model related to monocrystalline films exhibiting grain size close to thickness. The size effects on the resistivity of evaporated palladium films [88] can be fitted quite satisfactorily by Equation 64 and yields a physically reasonable value of about 1.7 for $M_{\rm m}(t,p)$. In sharp constrast to these results, Borodziuk-Kulpa *et al.* [50] reported anomalously large size effects on the resistivity of thin vanadium films and obtained a very large value of about 17 for the $M_{\rm m}(t,p)$ function. Such a high value cannot be attributed to grain-boundary scattering alone but can perhaps be understood in terms of additional imperfections depending linearly on thickness as suggested by these authors. However thermal ageing at 570 K does not induce a marked decrease of the resistivity. Here the interpretation would be more significant if additional structural studies were made. Structural studies may also be of interest in analysing the results on indium films [44] or tin films [46] since the authors assumed that, for

thinner films, the grains exhibit a columnar shape [46] with grain size that remains equal to film thickness [44] and that as the film thickens the grain size becomes nearly constant. Such films can then be interpreted successively in terms of bidimensional and three-dimensional models of grains. Results on the thickness dependence of the electrical resistivity and its TCR of annealed thin copper films [89] agree well with Equation 71 and yield the following pair of values of the parameters ($t = 0.9, p = 0.6$) and ($t = 0.8, p = 0.9$).

Tochitskii and Belyavskii [71] studied grain-boundary scattering on various metal films of given thicknesses. Effect of substrate temperature T_{sub} on film structure was investigated and the grain size was evaluated by transmission electron microscopy (TEM) techniques. The grain size dependence of the resistivity was compared with the Mayadas–Shatkzes (MS) model in order to determine the reflection coefficient r at grain boundaries, which is related to the transmission coefficient t defined in multidimensional models by

$$\ln(1/t) \approx r(1-r)^{-1} \qquad (101)$$

The grain-boundary contribution to resistivity was evaluated by means of Matthiessen's rule. The resistivity ratio ρ_g^*/ρ_0 was found to take values in the range 1.10 to 2.17. It should be noticed that as the grain size increases with increasing T_{sub} the film exhibits successively polycrystalline and monocrystalline structure. Then the resistivity ρ_g^* cannot be connected with the resistivity ρ_g of an infinitely thick film but with the extra resistivity of a given film of particular thickness deposited on a substrate maintained at high temperature and exhibiting a monocrystalline structure, i.e.

$$\rho_g^* = 1.144\,(\lambda_0/D_g)\ln(1/t) \qquad (102)$$

However in the absence of complete resistivity data, no conclusion can be drawn.

Ghosh and Pal [54] studied the resistivity and TCR of thin evaporated nickel films and obtained a reasonable value ($\rho_\infty \approx 2\rho_0$) for the resistivity ρ_∞ of an infinitely thick film in correlation with the fine-grained structure revealed by electron micrographs and diffraction patterns. However the product $\rho_\infty\beta_\infty$ was found to depart from the law (Equation 55). Since Relation 55 is also valid when the contribution ρ_I to the film resistivity is temperature-independent, this departure can be attributed to random TCR data which make the

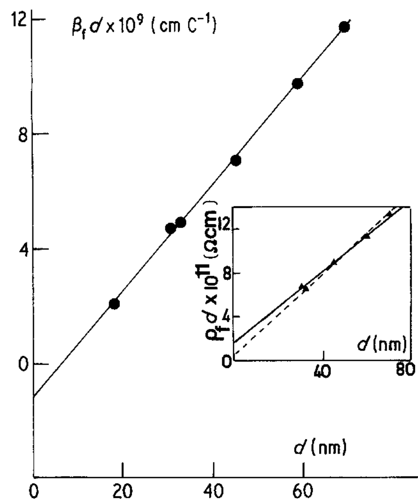

Figure 9 A plot of $\beta_f d$ against d for nickel films. In the inset is shown the modified $\rho_f d$ against d plot (Angadi and Udachan [49]): full line, experimental data; broken line, three-dimensional model.

thickness dependence of the TCR not clear. Angadi and Udachan [49] reported results on size effects on resistivity and TCR of evaporated nickel films. They analysed their data in terms of the MS model assuming that $d \approx D_g$ over the thickness range 6 to 25 nm and $d < D_g$ for thicker films. Moreover a perfect linear relation between $\beta_f d$ and d is verified. However since a quite high value of ρ_∞ with respect to ρ_0 was deduced ($\rho_\infty \approx 2.8\rho_0$) and since the Relation 55 was found to be approximately satisfied (i.e. $\beta_0 \approx 3\beta_\infty$), the data may also be understood for thinner films in the light of the monocrystalline model and for $d >$ 20 nm in the light of the three-dimensional model of grain boundaries. We have made an attempt to fit their data in terms of Equation 64 and

$$\beta_{fp}/\beta_{gp} = 1 - k^{-1}\ln(1/p)M_p(\nu) \qquad (103)$$

derived from Equation 66 when $k^{-1}\ln(1/p)M_p(\nu)$ takes small values by modifying (inset of Fig. 9) the slope of their $\rho_f d$ against d plot in order to obtain a resistivity ratio ρ_∞/ρ_0 strictly equal to 3. The straight lines of Fig. 9 exhibit behaviours in agreement with the three-dimensional model and yield p values of about 0.4 from the resistivity plot and about 0.7 from the TCR plot. However analysing their data on the basis of the columnar model should certainly lead to similar results. Thus this experimental work clearly shows how useful are the structural studies to corroborate theoretical predictions with experimental results.

In the majority of experimental work devoted

to resistivity and TCR no attempt has been made to explain partially the role of grain boundaries and/or imperfections by examining the annealing effect. The first evidence of grain-boundary migration on annealing was provided by Van Gurp [20] who studied the grain size increase as a function of annealing temperature (AT) and evaluated the grain-boundary resistivity in terms of the MS model. Similarly Uda *et al.* [8] investigated by scanning electron microscopy (SEM) the annealing behaviour of molybdenum films. The AT dependence of D_g was found to be well correlated with resistivity dependence. However their results were not connected with a defined restructuration process. Tellier [23] showed that annealing in polycrystalline zinc films results in both grain migration and surface reordering, and this interpretation was sustained by measurement, before and after annealing, of film resistivity and TCR. Longbrake and Brient [90] used the MS model to determine the change in the reflection coefficient r (i.e. transmission coefficient t) on annealing. However as the grain size was assumed to remain constant during annealing, an alternative interpretation of the observed increase in grain parameter ν is that D_g increases slightly on annealing. Narayandas *et al.* considered the thickness dependence of defect density in silver films [91] and copper films [92] and interpreted annealing results on the basis of Vand's theory [93]. Activation energy was found to vary over the range 1.1 to 1.5 eV for silver films and over the range 1.27 to 1.43 eV for copper films. After annealing ρ_∞ and $1/\beta_\infty$ were only about 10% greater than bulk values. As the structure of silver films was found to be grained, a zero value of p was assumed. Since surface reordering generally takes place in the first stage of annealing and results in partially specular scattering, a more realistic fit would have been achieved using the theory of monocrystalline film and undertaking a simultaneous structural study.

Narashimha Rao *et al.* made measurements of thermopower, resistivity and TCR on annealed copper [89] and silver [94] films and suggested a thickness dependence of the energetic terms U and V which decreased by about 20% with increasing thickness. But examination of their data by Tellier and Tosser [37] has given evidence against the adequateness of the monocrystalline model to describe the resistivity and TCR behaviour. This interpretation was sustained by satisfactory fits of the variation in ΔS_{0m} and S_{fm}/S_0 with σ_{fm}/σ_0 yielding constant values for U and V. Damodara Das and Mohanty [95] studied the thermopower of β-tin films between 300 and 425 K. The films exhibited a fibrous structure with grain boundaries parallel to the substrate. No theoretical equations have been derived for a such fibrous structure but it is reasonable to expect the main conclusions related to polycrystalline or columnar films to apply here. The thickness dependence of thermopower was found to satisfy a linear law for k up to 0.1. This result agrees well with theoretical predictions of columnar and polycrystalline models, that effectively for relatively small ν the linearized forms of TCR ratio (Equation 66 and 71) are still valid for small $k (k \geqslant 0.1)$.

Large contributions to thermopower in thin metal films can be provided by the existence of large concentration of imperfections frozen in films. Hence some studies [14, 15, 72, 83–86] have been devoted to annealing effects on resistivity, TCR and thermopower. Sugawara *et al.* analysed the annealing behaviour of thermopower of thin copper films against copper wires [96] and thin gold films against lead–copper wires [72]. They neglected grain-boundary scattering and interpreted their data in terms of the Nordheim–Gorter rule by plotting $\rho_f^* \Delta S_0^*$ as a function of ρ_s. The fact that $\rho_f^* \Delta S_0^*$ depends linearly on ρ_s can be interpreted in terms of three alternative equations, and hence as discussed earlier the choice of the theoretical equation can cause large errors in S_s and U. Moreover the contribution ρ_I to resistivity was assumed to be independent of thickness even if the relatively marked dispersion of point data after annealing has required a least-squares method to determine the surface scattering parameter. In the case of gold films [72] the energetic parameter U has been assumed to vary on annealing but the changes of ρ_I and perhaps S_I on annealing were not clearly established, so that a complete conclusion cannot be drawn. Leonard and Lin [85] used the Nordheim–Gorter rule to determine the component S_s of thermopower by plotting ΔS_0^* against $1/\rho_f^*$. They obtained two straight-line segments with slope of opposite sign. Since a surface restructuration process which requires small activation energy certainly occurs at lowest AT, they considered the linear segment corresponding to this temperature range to estimate S_I from the ordinate intercept of the ΔS_0^* against $1/\rho_f^*$ plot. Then the evaluated S_I value is

probably concerned with as-deposited films since the existence of two intersecting straight lines seems to indicate that S_I varies on annealing as expected when annihilation of various structural defects arises at different annealing stages.

Suri *et al.* [14, 15, 86] have undertaken comprehensive studies of annealing effects on resistivity, TCR, thermopower and Hall coefficient of monocrystalline copper films. The conductivity ratio, σ^*_{fm}/σ_0, dependence of the difference ΔS^*_{0m} in thermopowers was found to deviate from a linear law. It could be advanced, as suggested by Suri *et al.*, that the observed behaviour is due to the thickness-dependent contribution of imperfection, in good agreement with the marked effect of annealing. Variations of the Hall coefficient and $\rho^*_f\beta^*_f$ with thickness showed an excellent quantitative fit with Equation 59 indicating that ρ_I is temperature-independent.

Wedler and Chander [88] studied the size effect on resistivity and thermopower of thin palladium films annealed at 300 and 440 K. The resistivity of an infinitely thick film annealed successively at 300 and 440 K was respectively found to deviate markedly ($\rho_\infty \approx 2.2\rho_0$) and slightly ($\rho_\infty \approx 1.15\rho_0$) from the bulk value indicating that for AT = 300 K the contribution ρ_I to resistivity remains significant. After annealing at 440 K the film thermopower approaches the bulk value and a linear relation between dS^*_{fm} and d was approximately verified. However, surprisingly, a plot of their data for thinner films in the form S^*_{fm} against d can also be described by a linear relation (Fig. 10) even if, for AT = 300 K, ρ_I is large with respect to ρ_0 and thus makes the supplementary condition of validity of Equations 96, namely $M_m(t,p)(\rho_I + \rho_0)/k\rho_0 < 1$, not completely fulfilled. Using Equation 96 leads to SV values of about $5\,\mu V\,K^{-1}$ for films annealed at 300 K and about $4.6\,\mu V\,K^{-1}$ for films annealed at 440 K. The values of S_I($S_I \approx 10.8\,\mu V\,K^{-1}$ for AT = 300 K, $S_I \approx 15\,\mu V\,K^{-1}$ for AT = 440 K) calculated from Equation 96 assuming that $S_0 = -9.3\,\mu V\,K^{-1}$ depend slightly on annealing temperature; this dependence may be due to small errors in the evaluation of $(\rho_I + \rho_0)$ and $M_m(t,p)$ for films annealed at 440 K. The thermopower data related to thicker films also fitted a linear relation as predicted by Equation 94 and yielded $SV = 4.5\,\mu V\,K^{-1}$ for AT = 300 K and $SV = 6.1\,\mu V\,K^{-1}$ for AT = 440 K, in fair agreement with previous values. Unfortunately the values of the component

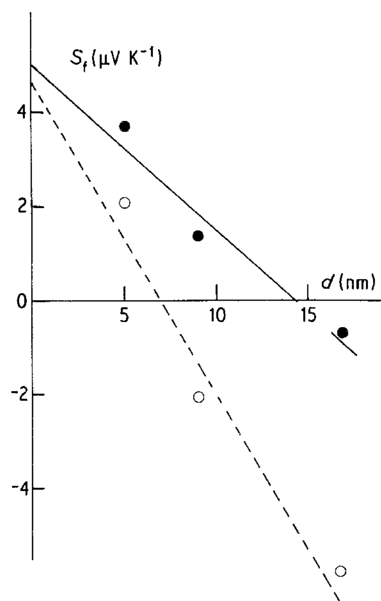

Figure 10 A plot of S_{fm} against k for thinner palladium films (Wedler and Chander [88]): full line, AT = 300 K; broken line, AT = 440 K.

S_I of thermopower evaluated after annealing at 300 and 440 K differ from those deduced for thinner films. This point is not understood and may be due to a thickness-dependent concentration of some defects. It is then convenient to perform careful structural studies to obtain consistent S_I values.

8. Conclusion

The significant fact to emerge from the experimental studies of defect effects on transport properties of thin films is the difficulty of separating the imperfection effects from size effects due to grain-boundary or suface scattering.

Generally resistivity and TCR data are in agreement with grain-boundary models. Moreover some results on resistivity recovery can be understood on the basis of grain-boundary models. Difficulties arise when we are concerned with the thermopower of films where a high concentration of imperfections is present. Experimental work does not establish clearly that the components S_I, S_s and S_g of thermopower can be regarded as intrinsic parameters. In contrast, changes of S_I on annealing or with thickness have been observed in some experimental work. Evaluation of V from the thickness dependence of the thermopower or difference in thermopowers does not establish without ambiguity that the energetic parameter

V related to the bulk thermopower S_0 varies with thickness or on annealing. It may be remarked that the determination of the imperfection contribution to the thermopower is generally seriously altered by the lack of information about the restructuration processes caused by thermal ageing and about the exact film structure.

References

1. J. M. ZIMAN, "Electrons and phonons" (Oxford University Press, London, 1962).
2. R. W. HOFFMANN, *Phys. Thin Films* **3** (1966) 211.
3. K. ABDELMOULA, B. PARDO, C. PARISET and D. RENARD, *Thin Solid Films* **62** (1979) 273.
4. T. T. SHENG, R. B. MARCUS, F. ALEXANDER and W. A. REED, *ibid.* **14** (1972) 289.
5. C. B. McDOWELL and T. C. PILKINGTON, *J. Appl. Phys.* **42** (1971) 7.
6. R. ABERMANN and R. KOCH, *Thin Solid Films* **66** (1980) 217.
7. H. T. G. NILSSON, B. ANDERSSON and S. E. KARLSSON, *ibid.* **63** (1979) 87.
8. K. UDA, Y. MATSUSHITA and S. I. TAKASU, *J. Appl. Phys.* **51** (1980) 1039.
9. M. MURAKAMI, *Thin Solid Films* **59** (1979) 105.
10. J. A. THORNTON and D. W. HOFFMANN, Technical Report SR 79 135 (Ford Motor Co., USA, 1979).
11. K. KINOSITA, *Thin Solid Films* **12** (1972) 17.
12. P. PETROFF, T. T. SHENG, A. K. SINHA, G. A. ROZGONYO and F. B. ALEXANDER, *J. Appl. Phys.* **6** (1973) 2545.
13. S. SEN, R. K. NANDI and S. P. SEN GUPTA, *Thin Solid Films* **48** (1978) 1.
14. R. SURI, A. P. THAKOOR and K. L. CHOPRA, *J. Appl. Phys.* **46** (1975) 2574.
15. *Idem, Solid State Commun.* **18** (1976) 605.
16. K. KAWAKITA, *Jpn. J. Appl. Phys.* **13** (1974) 1940.
17. R. SURI and K. L. CHOPRA, *Thin Solid Films* **36** (1976) 47.
18. J. M. HERAS and E. E. MOLA, *ibid.* **36** (1976) 75.
19. J. C. BLAIR, C. R. FULLER, P. B. GHATE and C. T. HAYWOOD, *J. Appl. Phys.* **43** (1972) 307.
20. G. J. VAN GURP, *J. Appl. Phys.* **46** (1975) 1922.
21. A. GANGULEE, *ibid.* **43** (1972) 3943.
22. S. K. SHARMA and O. P. BAHL, *Thin Solid Films* **6** (1970) 239.
23. C. R. TELLIER, *ibid.* **51** (1978) 53.
24. S. D. MUKHERJEE, "Reliability and Degradation", edited by M. J. Howes and D. V. Morgan (Wiley, Chicester, 1981) p. 10.
25. C. R. TELLIER and A. J. TOSSER, *Electrocomp. Sci. Technol.* **3** (1976) 85.
26. R. E. HUMMET and A. J. GEIER, *Thin Solid Films* **25** (1975) 335.
27. J. P. CHAUVINEAU and C. PARISET, *Surf. Sci* **36** (1973) 155.
28. C. PARISET and J. P. CHAUVINEAU, *ibid.* **47** (1975) 543.
29. E. H. SONDHEIMER, *Adv. Phys.* **1** (1952) 1.
30. A. A. COTTEY, *Thin Solid Films* **1** (1967–68) 297.
31. R. G. CHAMBERS, *Proc. R. Soc.* **202 A** (1950) 378.
32. K. L. CHOPRA, "Thin Film Phenomena" (McGraw-Hill, New York, 1968).
33. J. E. PARROTT, *Proc. Phys. Soc.* **85 C** (1965) 1143.
34. G. BRANDLI and P. COTTI, *Helv. Phys. Acta* **38** (1965) 801.
35. S. SOFFER, *J. Appl. Phys.* **38** (1967) 1710.
36. M. S. P. LUCAS, *ibid.* **36** (1965) 1632.
37. C. R. TELLIER and A. J. TOSSER, "Size Effects in Thin Films" (Elsevier, Amsterdam, 1982) chap I.
38. A. F. MAYADAS and M. SHATZKES, *Phys. Rev. B* **1** (1970) 1382.
39. F. WARKUSZ, *Electrocomp. Sci. Technol.* **5** (1978) 197.
40. *Idem, Acta Phys. Polon.* **54 A** (1978) 31.
41. C. R. TELLER, C. R. PICHARD and A. J. TOSSER, *Thin Solid Films* **61** (1979) 349.
42. C. R. PICHARD, C. R. TELLIER and A. J. TOSSER, *ibid.* **62** (1979) 189.
43. C. R. TELLIER and A. J. TOSSER, *ibid.* **70** (1980) 225.
44. A. K. PAL and S. CHAUDHURI, *J. Mater. Sci.* **11** (1976) 872.
45. E. E. MOLA, J. BORRAJO and J. M. HERAS, *Surf. Sci.* **34** (1973) 561.
46. A. K. PAL and PARAMITA SEN, *J. Mater. Sci.* **12** (1977) 1472.
47. B. SINGH, C. C. LING and N. A. SURPLICE, *Thin Solid Films* **23** (1974) S50.
48. *Idem, ibid.* **24** (1974) S27.
49. M. A. ANGADI and L. A. UDACHAN, *ibid.* **79** (1981) 149.
50. A. BODODZIUK-KULPA, B. STOLECKI and C. WESOLOWSKA, *J. Mater. Sci.* **16** (1981) 1961.
51. R. D. BARNARD, "Thermoelectricity in Metals and Alloys" (Taylor and Francis, London, 1972) chaps. 2, 3 and 6.
52. L. OURBYA, C. R. TELLIER and A. J. TOSSER, *J. Mater. Sci.* **16** (1981) 2287.
53. M. HUBIN and J. GOUALUT, *C. R. Acad. Sci. Paris B* **275** (1972) 195.
54. C. K. GHOSH and A. K. PAL, *J. Appl. Phys.* **51** (1980) 2281.
55. S. K. BANDYOPADHAY and A. K. PAL, *J. Phys. D: Appl. Phys.* **12** (1979) 953.
56. V. V. R. NARASIMHA RAO, S. MOHAN and P. JAYARAMA REDDY, *ibid.* **9** (1976) 89.
57. HO-HUAN HU and W. F. LEONARD, *J. Appl. Phys.* **44** (1973) 5324.
58. W. F. LEONARD and HO-YUAN HU, *ibid.* **44** (1973) 5320.
59. C. R. PICHARD, C. R. TELLIER and A. J. TOSSER, *Phys. Status Solidi a* **65** (1981) 327.
60. C. R. TELLIER, C. R. PICHARD and A. J. TOSSER *Thin Solid Films* **76** (1981) 129.
61. C. R. TELLIER, A. J. TOSSER and L. HAFID, *J. Mater. Sci.* **15** (1980) 2875.
62. J. B. THOMPSON, *Thin Solid Films* **18** (1973) 77.
63. C. R. TELLIER, C. R. PICHARD and A. J. TOSSER, *J. Mater. Sci.* **17** (1982) 290.

64. C. R. PICHARD, A. J. TOSSER and C. R. TELLIER, *ibid.* **16** (1981) 451.
65. C. R. PICHARD, A. J. TOSSER, C. R. TELLIER and K. C. BARUA, *ibid.* **16** (1981) 2480.
66. E. H. SONDHEIMER, *Phys. Rev.* **80** (1950) 401.
67. V. HALPERN, *J. Phys. F: Metal Phys.* **1** (1971) 608.
68. K. L. CHOPRA, R. SURI and A. P. THAKOOR, *J. Appl. Phys.* **48** (1977) 358.
69. P. MICHON, *Thin Solid Films* **16** (1973) 335.
70. U. ADMON, A. BAR-OR and D. TREVES, *J. Appl. Phys.* **44** (1973) 2300.
71. E. I. TOCHITSKII and N. M. BELYAVSKII, *Phys. Status Solidi a* **61** (1980) K21.
72. H. SUGAWARA, T. NAGANO and A. KINBARA, *Thin Solid Films* **21** (1974) 33.
73. K. L. CHOPRA and A. P. THAKOOR, *J. Appl. Phys.* **49** (1978) 2855.
74. C. R. PICHARD, C. R. TELLIER and A. J. TOSSER, *J. Mater. Sci.* **15** (1980) 2236.
75. P. M. HALL, *Appl. Phys. Lett.* **12** (1968) 212.
76. F. WARKUSZ, *J. Phys. D: Appl. Phys.* **11** (1978) 689.
77. N. JAIN and R. SRIVASTAVA, *J. Mater. Sci. Lett.* **1** (1982) 397.
78. C. R. TELLIER, A. J. TOSSER and L. HAFID, *Appl. Phys.* **23** (1980) 357.
79. G. WEDLER and W. WIEBAUER, *Thin Solid Films* **28** (1975) 65.
80. B. STOLECKI, A. BORODZIUK-KULPA and C. WESOLOWSKA, *ibid.* **56** (1979) 299.
81. C. R. TELLIER, C. R. PICHARD, A. J. TOSSER and L. HAFID, *ibid.* **94** (1982) 93.
82. C. R. TELLIER, L. HAFID and A. J. TOSSER, *Rev. Phys. Appl.* **15** (1980) 1573.
83. A. P. THAKOOR, R. SURI, S. K. SURI and K. L. CHOPRA, *Appl. Phys. Lett.* **26** (1975) 160.
84. HO-YUAN YU and W. F. LEONARD, *Thin Solid Films* **20** (1974) 383.
85. W. F. LEONARD and S. F. LIN, *ibid.* **11** (1972) 273.
86. A. P. THAKOOR, R. SURI, S. K. SURI and K. L. CHOPRA, *J. Appl. Phys.* **46** (1975) 4777.
87. P. A. B. TOOMBS and P. BENNETT, *ibid.* **39** (1968) 2948.
88. G. WELDER and R. CHANDER, *Thin Solid Films* **65** (1980) 53.
89. V. V. R. NARASIMHA RAO, S. MOHAN and P. JAYARAMA REDDY, *J. Phys. D: Appl. Phys.* **9** (1976) 89.
90. R. L. LONGBRAKE and S. J. BRIENT, *Thin Solid Films* **43** (1977) 343.
91. K. NARAYANDAS, M. RADHAKRISHNAN and C. BALASUBRAMANIAN, *ibid.* **67** (1980) 357.
92. K. NARAYANDAS, M. RADHAKRISHNAN and C. BALASUBRAMANIAN, *Electrocomp. Sci. Technol.* **9** (1982) 171.
93. V. VAND, *Proc. Phys. Soc.* **55** (1943) 222.
94. V. V. R. NARASIMHA RAO, S. MOHAN and P. JAYARAMA REDDY, *Thin Solid Films* **42** (1977) 283.
95. V. DAMODARA DAS and JYOTISH CHANDRA MOHANTY, *J. Appl. Phys.* **54** (1983) 977.
96. H. SUGAWARA, T. NAGANO, K. UOZUMI and A. KINBARA, *Thin Solid Films* **14** (1972) 349.

Received 29 May
and accepted 19 July 1984